PCCP

Physical Chemistry Chemical Physics

An international journal

www.rsc.org/pccp

Volume 8 | Number 2 | 14 January 2006 | Pages 197–312

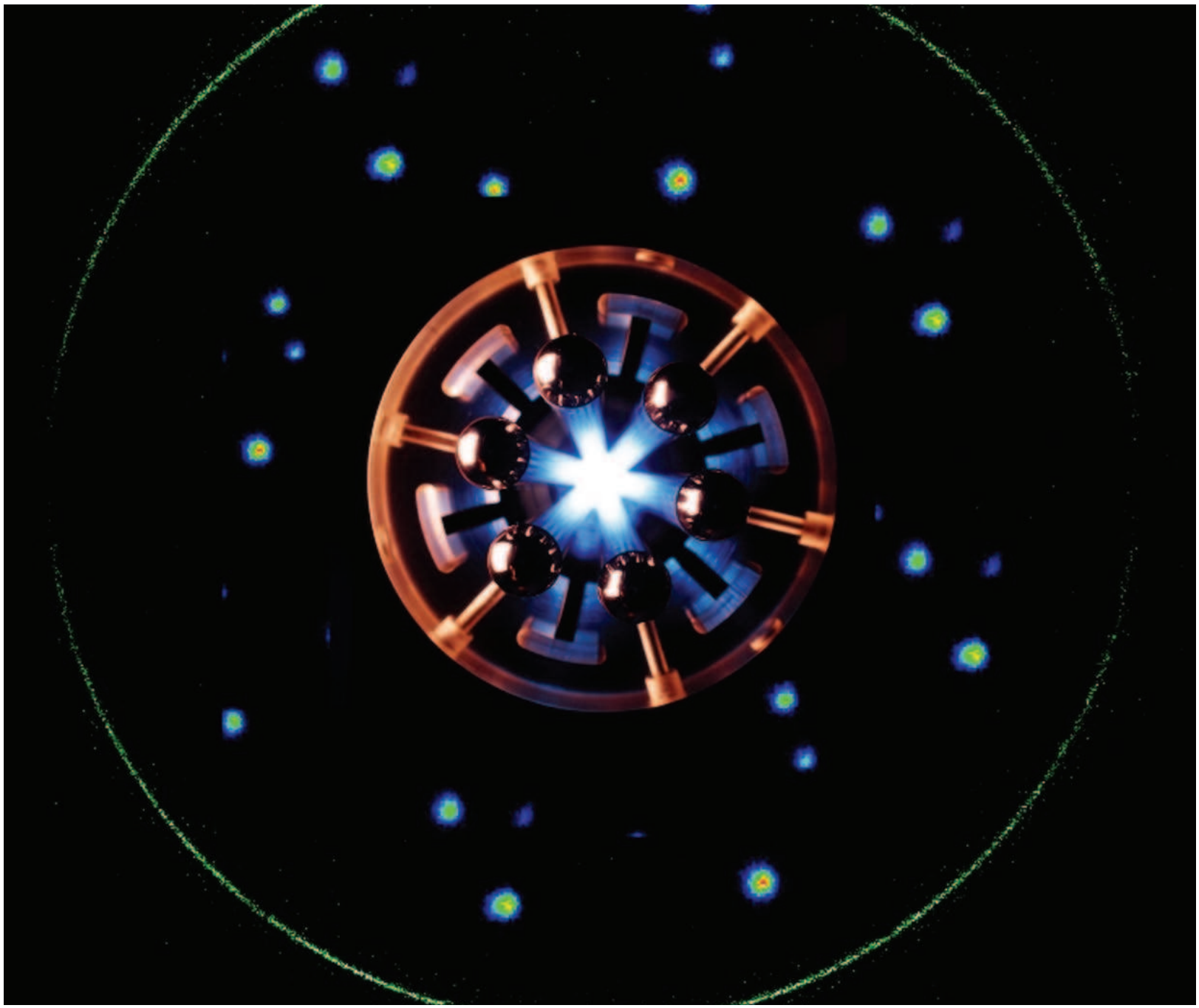

ISSN 1463-9076

1463-9076(2006)8:2;1-5

High resolution slice imaging of a molecular speed distribution

M. Laura Lipciuc, Joost B. Buijs and Maurice H. M. Janssen*

Received 15th November 2005, Accepted 24th November 2005
First published as an Advance Article on the web 1st December 2005
DOI: 10.1039/b516186j

High resolution slice imaging experiments are reported measuring the speed distribution of molecular fragments, recoiling at a most probable speed v_{mp}, with a full-width-half-maximum (FWHM) speed resolution near the permille level: $FWHM_v/v_{mp} = 1.9 \times 10^{-3}$. We implemented a high resolution single-particle slice imaging detector and used a two-colour resonance-enhanced multi-photon ionisation (REMPI) scheme to reduce broadening of the speed distribution due to the electron kick. The results on the measurement of the CD_3 speed distribution from photolysis of CD_3I show that it is possible to image the three-dimensional speed distribution at a resolution down to $FWHM_v = 6.7$ m s^{-1}, when the fragment has an absolute speed of $v_{mp} = 3473$ m s^{-1}. The new experiments demonstrate the potential of slice imaging to measure with high resolution the three-dimensional speed distribution of a cloud of molecules.

1. Introduction

The application of imaging techniques in the field of chemical reaction dynamics has expanded vastly since the first demonstration of ion imaging by Chandler and Houston in 1987.[1] The velocity resolution obtained in imaging experiments has improved since by the introduction of two variants, velocity map imaging in 1997[2] and slice imaging in 2001[3] and 2003.[4,5] The initial motivation for the development of slice imaging was to eliminate constraints with respect to cylindrical symmetry in the experiment, which was a prerequisite to reconstruct from the measured two-dimensional projected data the three-dimensional velocity distribution. The slice imaging variant facilitates the analysis and made the Abel-inversion of projected images superfluous. Furthermore, it turns out that the slice imaging technique provides a better velocity resolution compared to the conventional velocity map imaging technique.[6]

Besides the improvements in ion optics there have been various developments over the last decades to improve the spatial resolution of the detection system. The detector is usually a charge-coupled-device (CCD) camera imaging the light spots from a phosphor screen which are produced by electrons at the backside of a micro-channel-plate (MCP). Light spots on the phosphor screen from individual ion events hitting a double (Chevron-type) MCP vary typically between 50–150 μm in diameter.[7,8] The spot size depends on the MCP pore size, the phosphor deposition process, the MCP–phosphor (anode) distance and the specific distribution of electron trajectories from MCP to anode. To improve the spatial resolution of intensifiers, centroiding techniques have been developed two decades ago in the field of astronomy and particle physics.[9,10] The optimisation of centroiding algorithms and the reduction of fixed pattern noise for event counting have been well studied in the past, see *e.g.* the review by Suhling *et al.*[11] Tremsin, Siegmund and coworkers[12] have pushed the resolution of centroiding techniques to the limit of the diameter of the entrance pore of a MCP and demonstrated 7 μm spatial resolution. Event counting and centroiding techniques were introduced initially in the chemical dynamics field by Ashfold, Whitaker and coworkers[13] and Houston and coworkers.[14] Very recently, Suits and coworkers[15] applied centroiding algorithms to obtain subpixel resolution in slice imaging experiments using a low pixel number standard video CCD camera.

In this paper we present the first results using slice imaging of photofragments to measure the velocity distribution with a relative speed resolution, $\Delta v/v$, near the 10^{-3} level. Photodissociation of CD_3I molecules, followed by slice imaging of CD_3 fragments is reported where a combination of experimental improvements enables us to obtain high resolution images of the speed distribution of the CD_3 fragment. The results reported here demonstrate that with slice imaging it is possible to measure the speed distribution of molecules at high resolution, which may be of interest for instance to characterise the speed distribution of clouds of cold molecules.[16]

2. Experimental

The experimental setup has been described in detail before.[17–19] Here we give a brief description focusing on the improvements made to obtain high resolution sliced images. A 20% mixture of CD_3I in Kr is supersonically expanded through a nozzle and skimmed before it enters a buffer chamber, traverses the hexapole chamber and finally enters the imaging chamber. The imaging chamber has an electrostatic ion lens set-up with three cylindrical plates, the repeller plate (R), the extractor plate (E) and one extra lens (L), see Fig. 1. The molecular beam is focused on a 1 mm conically shaped hole in the repeller plate. In the ion lens the molecular beam is crossed with up to three different laser beams. A photolysis beam at 266 nm, with pulse energy of about 2–3 mJ, is focused on the molecular beam. At 90°, two counter-propagating laser beams cross. A UV beam around 334 nm excites the CD_3 photofragments *via* the 0_0^0 band of the $3p_z{}^2A_2'' \leftarrow\leftarrow 2p_z\tilde{X}^2A_2''$ two-photon

Laser Centre and Department of Chemistry, Vrije Universiteit, de Boelelaan 1083, 1081 HV Amsterdam, The Netherlands. E-mail: mhmj@chem.vu.nl

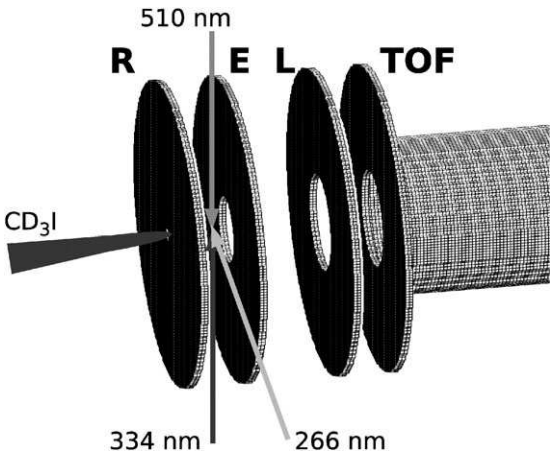

Fig. 1 Ion lens setup for high resolution slice imaging. A quantum state selected beam of CD_3I molecules is focused on a 1 mm conical aperture in the repeller plate (R) of an ion lens. The photolysis laser beam at 266 nm crosses at right angles with the molecular beam and two counter propagating probe laser beams at 334 nm and 510 nm. The ionised CD_3^+ photofragment is accelerated towards an extractor (E), passes an extra ion lens (L) and enters a time-of-flight (TOF) tube. At the end of the TOF-tube a chevron MCP detector with phosphor screen and large size CCD camera images the spatial distribution. The gain of the MCP is switched with a fast homebuilt HV gate.

transition. It is well known that the $3p_z{}^2A_2''$ intermediate state is predissociative.[20–22] The two-photon excited CD_3 photofragments can either absorb a third UV photon and ionise or they can absorb a visible photon at around 510 nm from the counter-propagating third laser beam. The wavelength of the visible laser beam is set to be just above the ionisation continuum and eject the electron with low kinetic energy.

The CD_3^+ ions are velocity mapped onto a position sensitive detector (MCP with phosphor screen and CCD camera). The detector is positioned at the end of a 35 cm time-of-flight (TOF) tube, which is in line with the molecular beam propagation direction. The MCP detector is gated with a homebuilt fast HV pulser.[19] The light of the phosphor screen is imaged on a 2048 by 2048 pixel frame CCD camera (PCO2000). The CCD camera is thermo-electrically cooled to reduce the dark current. A special software program reads out the large frame CCD camera in real time, typically every two laser shots (200 ms). The large frame image is analysed on the fly for events and the centroid of each event is obtained. We employ the centroiding strategy as suggested by Suhling and coworkers[23] to minimise fixed pattern noise and use the hybrid algorithm, a combination of centre-of-gravity centroiding and Gaussian centroiding. Typically, the number of events per frame varies between 0–10 events. For every detected event within a frame the centroided coordinates, with subpixel accuracy, are stored as well as the corresponding maximum intensity of the pixel of the event. The software updates, after every frame readout, the accumulated image with events located at the maximum pixel intensity to a computer screen. We accumulate frames until a sufficiently large number of events is obtained, see the results reported below.

3. Results and discussion

When CD_3 is photoionised with one-colour (2 + 1) REMPI around 334 nm the recoil kick, v_{kick}, on the ionic CD_3^+ fragment due to the electron is about v_{kick} = 21 m s^{-1}. The absolute speed of CD_3 fragments in the vibrational ground state correlating with I* atoms in the spin–orbit excited state, which is the dominant channel for photodissociation at 266 nm, is v_{mp} = 3473 m s^{-1}. The absolute speed was calibrated using conservation of energy and linear momentum in the dissociation and well known spectroscopic information on CD_3I and CD_3.[24] The internal rotational energy of a state-selected CD_3I (JK = 11) parent molecule E_{rot} (CD_3I) = 2.8 cm^{-1}, the rotational energy of the CD_3 (JK = 41) (the most populated state where the UV probe wavelength was set), E_{rot} (CD_3) = 93.6 cm^{-1}. We use the value of the dissociation energy, D_0 = 2.420 eV,[25] an ionisation energy IP = 9.838 eV,[26] a photon energy (for a quadrupled Nd:YAG photon at 266 nm) $E_{photolysis}$ = 4.658 97 eV and an iodine spin–orbit splitting energy of E(I*) = 0.942 68 eV. This means that the ultimate speed resolution that can be obtained in the absence of other broadening mechanisms will be limited by v_{kick}. For one-colour (2 + 1) REMPI of CD_3 this would give $FWHM_v/v_{mp}$ = 42/3473 ≈ 1.2×10^{-2}. Therefore, to obtain a resolution at the permille level a two-colour (2 + 1′) photoionisation process is needed to reduce the broadening from the electron kick. Pratt and coworkers reported (2 + 1′) photoelectron spectroscopy of the methyl radical.[27] They used the $4p_z{}^2A_2''$ ←← $2p_z\tilde{X}^2A_2''$ two-photon transition with a frequency doubled dye laser around 286 nm and the fundamental dye frequency for the one-photon ionisation. In our case we use the $3p_z{}^2A_2''$ ←← $2p_z\tilde{X}^2A_2''$ transition where one photon of the fundamental dye laser is not sufficient for ionisation. Therefore, a third laser was used to independently provide the visible photon for ionisation. The visible probe laser is set at 510 nm to just ionise CD_3 from the excited $3p_z{}^2A_2''$ intermediate state. Using the adiabatic IP = 9.838 eV, a two-photon $3p_z{}^2A_2''(J'K')$ = (41) ←← $2p_z\tilde{X}^2A_2''(J''K'')$ = (41) transition energy of 598 85.2 cm^{-1} we find a threshold wavelength for ionisation of about 513.8 nm. When the probe wavelength was scanned to slightly longer wavelength of 512–513 nm the enhancement by the visible probe reduced significantly. Therefore, in order to have a good enhancement from the visible probe beam we compromised and set the visible probe wavelength at 510 nm. With a visible photon at 510 nm the recoil kick is reduced to v_{kick} = 3.4 m s^{-1}.

We performed experiments using the UV and visible laser beams for (2 + 1′) ionisation, or blocking the visible beam and recording images, under exactly the same conditions, with the UV beam only for (2 + 1) ionisation. It was possible to optimise the spatial and temporal overlap of the UV and visible probe laser beams by maximising the enhancement of the CD_3^+ ion signal as measured by a photomultiplier recording the total light from the phosphor screen. The enhancement was very sensitive to the spatial alignment of the two probe laser beams, as all beams were focused down with lenses with focal distances of about 20–25 cm. The temporal overlap was set with a fast photodiode. Scanning the time delay between the two probe laser beams showed that the enhancement of the

CD_3^+ ion signal reduced when the two probe beams were delayed over about 2–3 ns. This is in accordance with the typical pulse width of Nd:YAG pumped dye lasers of about 5–7 ns.

The images that were obtained are represented in two different ways. The first representation is by plotting the accumulated events where each event is represented by a count at the position of the pixel with the maximum intensity. Such an image (denoted peak image, PI) has the dimensions of the large-frame CCD camera of 2048 by 2048 pixels. A second representation is made by using the data as accumulated by the on-the-fly centroiding. To select the optimal number of subpixels (which in principle can be done at arbitrary resolution) we take the diameter of the entrance pore of our MCP (10 μm) as the ultimate limit to the spatial resolution of our detector. This means that over the diameter of 42 mm of the MCP plate about 4200 pixels will provide 10 μm resolution. A larger number of pixels will not enhance the resolution. Therefore, the sub-binning is done with only two subpixels for each real pixel of the large-frame CCD camera. A centroided image (denoted CI) has a size of 4096 by 4096 pixels, and the total number of centroided pixels (16 megapixels) is enlarged by a factor of four compared to the total number of real pixels (4 megapixels).

To set the optimal voltages on our ion plates (V_R = 719 V, V_E = 626 V and V_L = 497 V, see Fig. 1) it was crucial that we updated after each frame readout (typically 200 ms equalling two laser shots) the PI image on the computer screen. Each image (4 megapixels) was searched by a very efficient algorithm for event spots. For each frame an image file accumulating the pixels with the peak intensity was updated and displayed in real time. The centroided coordinates and the peak intensity of each spot were stored as events in a text data file. Furthermore, a sub-window on the computer screen showed an enlarged part of the image with a fit of an integrated cut of the narrow ring of photofragments. In this way it was experimentally possible to optimise the voltages on the lenses to within 1–2 V. Also, the optimal slice delay time of the HV pulse on the MCP was set using the image displayed on the computer screen. As is reported elsewhere,[19] the homebuilt gate has an effective gain width of about 12–15 ns, depending on the total gain voltage on the MCP. The total spread in arrival time for the CD_3^+ fragments is about 220 ns for the extraction field strength of 55 V cm^{-1}. Once the optimal experimental conditions were set, data images were accumulated for up to 2 h. Under our laboratory conditions longer data acquisition times were not feasible due to a slow drifting away of the spatial overlap of the foci of the three laser beams. This was most clearly observed by the reduction in the enhancement of the ionisation signal due to the visible probe beam.

In Fig. 2 we show the PI image of the sliced three-dimensional velocity distribution of CD_3 using the two-colour (2 + 1′) ionisation scheme. For this image the total CD_3^+ ion signal with the visible beam present was more than double the ion signal from the 334 nm probe beam only. In Fig. 3 we show a 300 by 300 pixels cut of the centroided image (total image is 4096 by 4096) using the on-the-fly centroiding of the spots and two-colour (2 + 1′) REMPI. The total number of events in this cut of the image is 1784 counts.

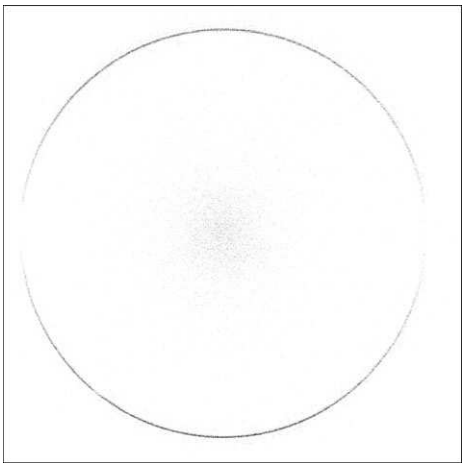

Fig. 2 Ion slice image using two-colour REMPI of CD_3^+. The total image size is 2048 by 2048 pixels, the total number of events is 43 043, the number of laser shots is about 72 000.

To determine the speed distribution we made a cut through the centre of the centroided image. In Fig. 4 we plot the speed distribution obtained from Fig. 3. As can be seen from Fig. 4(b) the speed distribution of the CI image obtained with two-colour (2 + 1′) REMPI contains a broader contribution resulting from one-colour (2 + 1) REMPI. On top of the broader peak is a much sharper peak from ions produced by the two-colour (2 + 1′) ionisation only. To calculate the speed resolution we fit through the experimental data a function $I(v) = I_{\text{one-colour}}(v) + I_{\text{two-colour}}(v)$, where each function $I_{n\text{-colour}}$ is represented by a Gaussian distribution. The best fit is found with $\text{FWHM}_{\text{two-colour}}$ = 6.7 m s^{-1} and $\text{FWHM}_{\text{one-colour}}$ = 35 m s^{-1}. So far we have not performed a detailed study of the expected lineshape at ultimate resolution. Such a study should include a careful analysis of the effect of the parent molecular beam velocity distribution, the spread due to the finite temporal width of the laser pulse and the MCP gain pulse. Furthermore, the molecular frame recoil of the photoelectron is anisotropic and this will be partially reflected in an anisotropic recoil in the laboratory frame. We already noticed in the initial experiments without the visible probe the effect on the

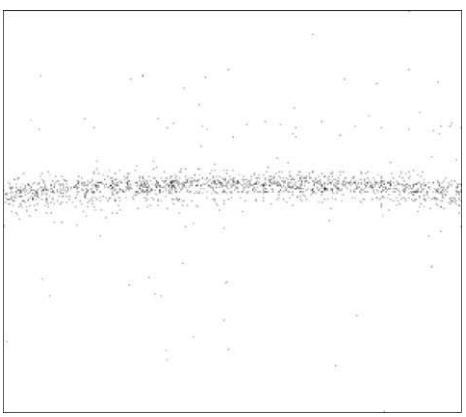

Fig. 3 Cut of the double centroided image of Fig. 2. The cut has a size of 300 by 300 pixels of a centroided image of 4096 by 4096 pixels. The total number of ion events is 1784.

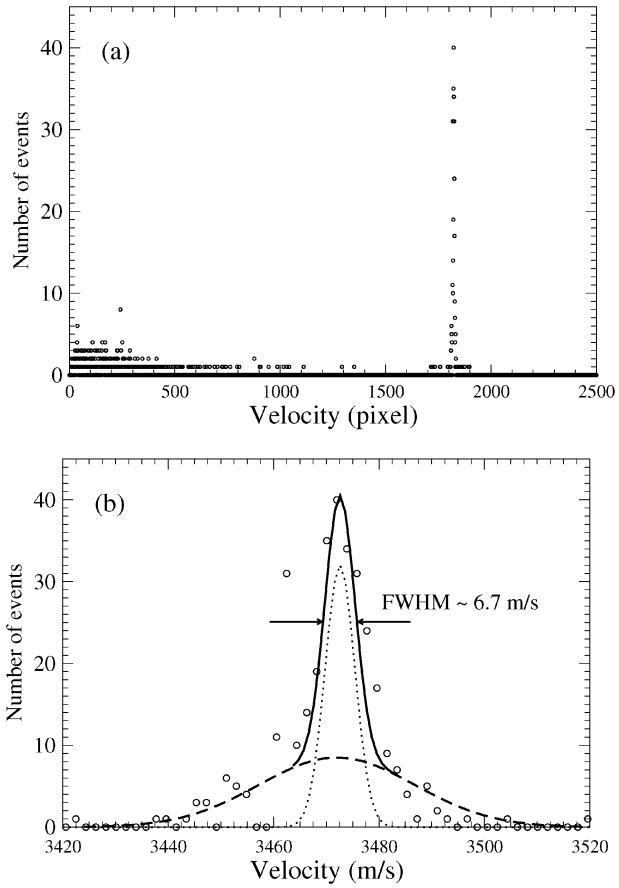

Fig. 4 (a) Velocity distribution (in pixels) of a vertical slice of 60 pixels wide of the centroided image. First the centre of the CI image was determined accurately, subsequently an angular integration over the 60 pixels wide slice of the upper ring was performed. The events near the centre of the image, *i.e.* at low velocity, are due to non-resonant ions produced by the 266 nm photolysis beam only. (b) Blow up of the region of interest showing the resolution of the speed distribution. The dashed curve is a single Gaussian distribution representing the contribution to the speed distribution from CD_3^+ produced in one-colour (2 + 1) REMPI with the 334 nm beam only. The dotted curve is a single Gaussian distribution representing the contribution to the speed distribution from CD_3^+ produced in two-colour (2 + 1′) REMPI with both the 334 nm and 510 nm beam. The solid line represents the sum of the dashed and dotted Gaussian curves. The narrow Gaussian has a $FWHM_v \approx 6.7$ m s^{-1}. The absolute velocity was calculated using a dissociation energy $D_0 = 2.420$ eV.

width of the speed distribution by rotating the polarisation of the UV probe from parallel to perpendicular to the polarisation direction of the photolysis beam. For the data presented here we simply used a Gaussian lineshape to represent the spread in the experimental speed distribution.

To the best of our knowledge the presently obtained resolution of $FWHM_v/v_{mp} = 6.7/3473 = 1.9 \times 10^{-3}$ is the highest resolution reported so far. Typically, (DC) slice imaging experiments have reported velocity resolutions around 1–2%.[4,5] Very recently, Suits and coworkers[15] reported slice imaging experiments of the D fragment from DBr photodissociation, where centroiding improved the velocity resolution from 0.68% to 0.5%. It is to be noticed here that the speed of the D atom in this experiment is about 16 430 m s^{-1}, so the velocity width obtained in this experiment is $FWHM_v$ = 82 m s^{-1}.

In our present experiment the velocity resolution may be limited by several factors of which the recoil kick from the electron appears still to be significant. Furthermore, the transversal velocity blurring from the state-selected molecular beam is estimated to be about 0.5–1.0 $\times$ 10^{-2} times the molecular beam velocity. For our seeded Kr beam this amounts to about 1.9–3.8 m s^{-1}. The width of the slice may still be a further limit to the resolution, and we are currently working on a faster HV switch so that the effective slice width is close to the time width of our lasers of about 5 ns. To achieve such thin slices it is important to operate with low capacitance MCP detectors. Therefore, to obtain very fast electrical gating it may be beneficial to use small size (18–25 mm diameter) MCP plates, with small pore size (2–5 μm) channels for good spatial resolution.

In conclusion, we have presented slice imaging experiments measuring the speed distribution of photofragments with a resolution near the permille level. We employed experimental improvements in large-frame CCD detectors with fast centroiding algorithms and two-colour (2 + 1′) REMPI. The results demonstrate the potential of slice imaging to measure the three-dimensional speed distribution at ultra-high velocity resolution.

Acknowledgements

This research has been financially supported by the councils for Chemical Sciences and Physical Sciences of the Dutch Organisation for Scientific research (NWO–CW, NWO–FOM). The authors would like to thank Mr Han Voet for the design of the fast HV MCP pulser, Mr Lex van der Gracht for the design of the fast ion optics voltage switcher, Mr Rob Kortekaas for building the ion lens. We like to acknowledge Dr A. S. Tremsin and Dr K. Suhling for helpful discussions on centroiding algorithms. We would like to thank Dr S. T. Pratt for stimulating discussions on two-colour photoionisation of methyl.

References

1 D. W. Chandler and P. L. Houston, *J. Chem. Phys.*, 1987, **87**, 1445.
2 A. T. J. B. Eppink and D. H. Parker, *Rev. Sci. Instrum.*, 1997, **68**, 3477.
3 C. R. Gebhardt, T. P. Rakitzis, P. C. Samartzis, V. Ladopoulos and T. N. Kitsopoulos, *Rev. Sci. Instrum.*, 2001, **72**, 3848.
4 D. Townsend, M. Minitti and A. G. Suits, *Rev. Sci. Instrum.*, 2003, **74**, 2530.
5 J. Lin, J. Zhou, W. Shiu and K. Liu, *Rev. Sci. Instrum.*, 2003, **74**, 2495.
6 D. Chestakov, S.-M. Wu, G. Wu, D. Parker, A. Eppink and T. Kitsopoulos, *J. Phys. Chem. A*, 2004, **108**, 8100.
7 A. Tremsin and O. H. W. Siegmund, *Rev. Sci. Instrum.*, 1999, **70**, 3282.
8 T. H. Hoenderken, C. W. Hagen, J. E. Barth, P. Kruit and G. O. Nützel, *J. Vac. Sci. Technol., B*, 2001, **19**, 843.
9 L. S. Barabasha, A. M. Baranov, G. B. Bondarenko, V. V. Chalysheva, B. A. Dolgoshein, I. A. Golutvina, V. A. Kantserov, A. V. Karpukhina, V. S. Khabarova, L. V. Komogorovaa, V. P. Konovalov, T. N. Konovalova, P. L. Nevsky, A. A. Popova, V. P.

Pugachevicha, A. V. Sumarokov and Y. A. Yatsunenkoa, *Nucl. Instrum. Methods Phys. Res., Sect. A*, 1985, **236**, 271.
10 M. K. Carter, B. E. Patchett, P. D. Read, N. Waltham and I. G. van Breda, *Nucl. Instrum. Methods Phys. Res., Sect. A*, 1991, **310**, 305.
11 K. Suhling, R. W. Airey and B. L. Morgan, *Nucl. Instrum. Methods Phys. Res., Sect. A*, 1999, **437**, 393.
12 A. Tremsin, J. V. Vallerga, O. H. W. Siegmund and J. S. Hull, *Proc. SPIE*, 2003, **5164**, 113.
13 L. J. Rogers, M. N. R. Ashfold, Y. Matsumi, M. Kawasaki and B. J. Whitaker, *Chem. Phys. Lett.*, 1996, **121**, 11645.
14 B.-Y. Chang, R. C. Hoetzlein, J. A. Mueller, J. D. Geiser and P. L. Houston, *Rev. Sci. Instrum.*, 1998, **69**, 1665.
15 W. Li, S. Chambreau, S. Lahankar and A. Suits, *Rev. Sci. Instrum.*, 2005, **76**, 63106.
16 M. S. Elioff, J. J. Valentini and D. W. Chandler, *Science*, 2003, **302**, 1940.
17 A. J. van den Brom, T. P. Rakitzis, J. van Heyst, T. N. Kitsopoulos, S. R. Jezowski and M. H. M. Janssen, *J. Chem. Phys.*, 2002, **117**, 4255.
18 M. H. M. Janssen, J. W. G. Mastenbroek and S. Stolte, *J. Phys. Chem. A*, 1997, **101**, 7605.
19 M. L. Lipciuc, A. J. van den Brom, L. Dinu and M. H. M. Janssen, *Rev. Sci. Instrum.*, 2005, in press.
20 D. W. Chandler, J. W. Thoman Jr, M. H. M. Janssen and D. H. Parker, *Chem. Phys. Lett.*, 1989, **156**, 151.
21 J. F. Black and I. Powis, *J. Chem. Phys.*, 1988, **89**, 3986.
22 A. J. van den Brom, M. L. Lipciuc and M. H. M. Janssen, *Chem. Phys. Lett.*, 2003, **368**, 324.
23 K. Suhling, R. W. Airey and B. L. Morgan, *Rev. Sci. Instrum.*, 2002, **73**, 2917.
24 D. H. Parker, Z. W. Wang, M. H. M. Janssen and D. W. Chandler, *J. Chem. Phys.*, 1989, **90**, 60.
25 This value was obtained from velocity map imaging measurements by A. J. van den Brom and M. L. Lipciuc partially reported in ref. 22 and A. J. van den Brom, PhD Thesis, Vrije Universiteit, Amsterdam, 2003.
26 M. Litorja and B. Ruscic, *J. Chem. Phys.*, 1997, **107**, 9852.
27 J. A. Bacon and S. T. Pratt, *Chem. Phys. Lett.*, 1999, **311**, 346.